

Exploring the Reactivity of Four-Coordinate PNPCoX with Access to Three-Coordinate Spin Triplet PNPCo

Michael J. Ingleson, Maren Pink, Hongjun Fan, and Kenneth G. Caulton*

Department of Chemistry, Indiana University, Bloomington, Indiana 47405

Received June 15, 2007

The compounds (PNP)CoX, where PNP is $(^i\text{Bu}_2\text{PCH}_2\text{SiMe}_2)_2\text{N}^-$ and X is Cl, I, N_3 , OAr, OSO_2CF_3 and N(H)Ar , are reported. Some of these show magnetic susceptibility, color, and ^1H NMR evidence of being in equilibrium between a blue, tetrahedral $S = 3/2$ state and a red, planar $S = 1/2$ state; the equilibrium populations are influenced by subtle solvent effects (e.g., benzene and cyclohexane are different), as well as by temperature. Attempted oxidation to Co(III) with O_2 occurs instead at phosphorus, giving $[\text{P(O)NP(O)}]\text{CoX}$ species. The single O-atom transfer reagent $\text{PhI}=\text{O}$ likewise oxidizes P. Even I_2 oxidizes P to give the pendant phosphonium species $(^i\text{Bu}_2\text{P(I)CH}_2\text{SiMe}_2\text{NSiMe}_2\text{CH}_2\text{P}^+\text{Bu}_2)\text{CoI}_2$ with a tetrahedral $S = 3/2$ cobalt; the solid-state structure shows intermolecular $\text{PI}\cdots\text{ICo}$ interactions. Attempted alkyl metathesis of PNPCoX inevitably results in reduction, forming PNPCo, which is a spin triplet with planar T-shaped coordination geometry with no agostic interaction. Triplet PNPCo binds N_2 (weakly) and CO (whose low CO stretching frequency indicates strong $\text{PNP} \rightarrow \text{Co}$ donor power), but not ethene or MeCCMe.

Introduction

Interest in the development of multidentate ligands originates from the fact that ligand characteristics, as much as the behavior inherent to the metal itself, dictate the chemical reactivity of transition metal complexes. One goal in ligand choice is to furnish multiple available coordination sites, resulting in space for more than one substrate molecule and, thus, in the substrate being coordinated in an essentially “barrierless” Lewis acid/base reaction. For the later transition elements, the question of a “high-spin” versus “low-spin” ground state arises, and therefore, the possible influence of spin state on chemical reactivity (both rate and thermodynamics) is also in question. For a variety of reasons, there is interest in the later 3d elements, with a goal of characterizing compounds with singly ($\text{M}-\text{R}$), doubly ($\text{M}=\text{CR}_2$, $\text{M}=\text{NR}$, and $\text{M}=\text{O}$), and triply bonded ($\text{M}\equiv\text{CR}$, $\text{M}\equiv\text{N}$) ligands.^{1–9} These are of interest as possible intermediates in olefin

polymerization, cyclopropanation/aziridination/oxidation, and group- or atom-transfer reactivity.^{10,11} Maintenance of a low metal-coordination number (vs dimerization or oligomerization) generally relies on bulky ligand substituents, which in turn influence reaction regiochemistry and substrate selectivity. Among the ligands studied, pincer ligands have appeal for relative ease of synthesis, modular character which permit systematic optimization, and a variety of spectroscopic probes, thus being especially “communicative”. Pincer ligands which are conjugated, either electron rich or electron poor, also show evidence of delocalization of their frontier orbitals when the metal/ligand complex is brought to low or high oxidation states, thus threatening the simple concept of metal oxidation state.^{12–15}

* To whom correspondence should be addressed. E-mail: caulton@indiana.edu.

- Jenkins, D. M.; Di Bilio, A. J.; Allen, M. J.; Betley, T. A.; Peters, J. C. *J. Am. Chem. Soc.* **2002**, *124*, 15336.
- Schebler, P. J.; Riordan, C. G.; Guzei, I. A.; Rheingold, A. L. *Inorg. Chem.* **1998**, *37*, 4754.
- Knijnenburg, Q.; Horton, A. D.; van der Heijden, H.; Kooistra, T. M.; Hetterscheid, D. G. H.; Smits, J. M. M.; de Bruin, B.; Budzelaar, P. H. M.; Gal, A. W. *J. Mol. Catal. A* **2005**, *232*, 151.
- Bart, S. C.; Hawrelak, E. J.; Lobkovsky, E.; Chirik, P. J. *Organometallics* **2005**, *24*, 5518.

- Hawrelak, E. J.; Bernskoetter, W. H.; Lobkovsky, E.; Yee, G. T.; Bill, E.; Chirik, P. J. *Inorg. Chem.* **2005**, *44*, 3103.
- Bart, S. C.; Lobkovsky, E.; Bill, E.; Chirik, P. J. *J. Am. Chem. Soc.* **2006**, *128*, 5302.
- Betley, T. A.; Peters, J. C. *J. Am. Chem. Soc.* **2004**, *126*, 6252.
- Matsunaga, P. T.; Hess, C. R.; Hillhouse, G. L. *J. Am. Chem. Soc.* **1994**, *116*, 3665.
- Betley, T. A.; Peters, J. C. *J. Am. Chem. Soc.* **2003**, *125*, 10782.
- Gibson, V. C.; Spitzmesser, S. K. *Chem. Rev.* **2003**, *103*, 283.
- Amisial Latasha, D.; Dai, X.; Kinney, R. A.; Krishnaswamy, A.; Warren Timothy, H. *Inorg. Chem.* **2004**, *43*, 6537.
- Knijnenburg, Q.; Hetterscheid, D.; Kooistra, T. M.; Budzelaar, P. H. M. *Eur. J. Inorg. Chem.* **2004**, 1204.
- Kooistra, T. M.; Hetterscheid, D. G. H.; Schwartz, E.; Knijnenburg, Q.; Budzelaar, P. H. M.; Gal, A. W. *Inorg. Chim. Acta* **2004**, *357*, 2945.

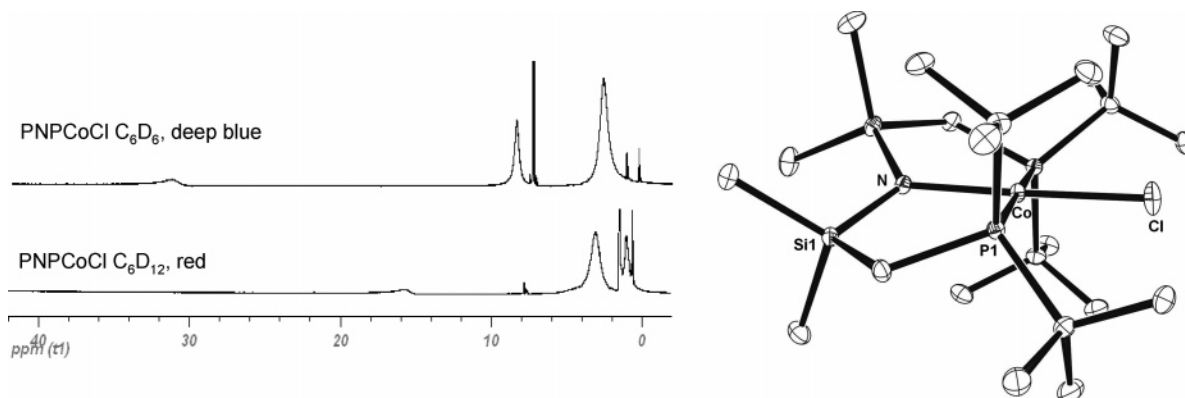


Figure 1. (Left) ^1H NMR (298 K) of complex **1** in C_6D_6 and in C_6D_{12} ; impurity peaks observed in both spectra can be assigned to residual solvent or silicone grease. (Right) ORTEP view (50% probabilities) of complex **1** (hydrogens are omitted for clarity). Selected bond lengths (\AA) and angles ($^\circ$): $\text{Co}-\text{N} = 1.9223(11)$, $\text{Co}-\text{Cl} = 2.2074(4)$, $\text{Co}-\text{P1} = 2.2898(4)$, $\text{Co}-\text{P2} = 2.2802(4)$, $\text{P1}-\text{Co}-\text{P2} = 177.414(15)$, $\text{N}-\text{Co}-\text{Cl} = 178.26(4)$, $\text{P1}-\text{Co}-\text{Cl} = 90.671(14)$.

The pincer ligand chosen in this work ($^t\text{Bu}_2\text{PCH}_2\text{SiMe}_2\text{N}^-$) has been previously demonstrated to carry enough bulk on phosphorus that it prohibits dimerization of $(\text{PNP})\text{RuX}$ by $\mu\text{-X}$ behavior, and thus enables the study of exceptionally low coordination numbers.^{16–18} In this sense, PNP shares some advantages of β -diketiminates, $\text{HC}(\text{CRNR}')_2^-$, when R and R' are bulky.¹⁹ However, because amide is one of the most potent π -donor ligands, PNP also makes a metal to which it is bound a stronger π -base, and indeed, highly unsaturated $(\text{PNP})\text{RuX}$ has demonstrated exceptional reducing ability for a d^6 , Ru^{II} species. Indeed, it can even be oxidized by 1-electron transfer to form isolable Ru^{III} species.¹⁶ It thus becomes of interest to study the physical properties and reactivity characteristics of 3d metals when bound to PNP.^{20,21} These metals are less expensive than Ru, they frequently show more rapid kinetics than 4d or 5d analogs, they often disregard the 18-electron rule, they have smaller d-orbital splittings, which often yield non-singlet spin states, they can prefer 1-electron (vs 2e for 4d and 5d analogs) redox changes, and their smaller size should aggravate the effects of steric bulk. The PNP ligand was thus anticipated to be a sufficiently potent donor that 1) 3-coordinate Co could be achieved and isolated and 2) the resulting species, even if far short of an 18 valence electron count, would be a reducing agent. In the work presented here, *each of these has been verified*, but with obvious subtle variations. Presented here is a general view of the chemistry of $(\text{PNP})\text{-CoX}$ species. A portion of this work has been previously communicated.^{22,23}

Results and Discussion

Synthesis and Solid-State Structures of PNPCoX ($\text{X} = \text{Cl, I, N}_3, \text{NH}(2,6\text{-Me}_2\text{-C}_6\text{H}_3)$). The combination of equimolar quantities of PNPMgCl /dioxane and anhydrous CoCl_2 in THF results, after 18 h, in the formation of a deep-blue solution, characteristic of a high-spin Co^{II} center in a tetrahedral environment. Recrystallization from deep-blue THF (or toluene) solutions, however, yielded red crystalline solids that upon being redissolved in THF or benzene became deep-blue solutions again; this process could be repeated numerous times. In contrast, dissolution of these red crystals

in saturated hydrocarbon solvents (pentane or cyclohexane) resulted in red solutions. *Solvatochromism* is a common indicator of a change in coordination number at the metal center, often caused by solvent coordination (and less frequently dimerization);^{24–26} to establish if this was the situation with this system, an excess (5–10 equiv) of THF (or C_6H_6) was added to a red pentane solution. This resulted in no significant color change, precluding solvent coordination. Dimerization was disfavored because of the substantial steric bulk provided by the ^tBu groups. A spin crossover between tetrahedral high-spin and square planar low-spin forms is an alternative, albeit a less common, phenomenon to account for the observed solvatochromism. Spin-state crossover has been previously suggested to be the origin of the thermochromism in the closely related compound $^{\text{Ph}}\text{PNPNiCl}$ ($^{\text{Ph}}\text{PNP} = [(\text{Ph}_2\text{PCH}_2\text{SiMe}_2)_2\text{N}]$), and square planar cobalt complexes ligated by the $^{\text{Ph}}\text{PNP}$ ligand are known, although they require stronger alkyl σ -donors to enforce spin pairing.²⁷

An X-ray diffraction study on the red crystals formed from cooling of a blue toluene solution revealed a monomeric complex, PNPCoCl , **1** (Figure 1) in a square planar environ-

- (14) Enright, D.; Gambarotta, S.; Yap, G. P. A.; Budzelaar, P. H. M. *Angew. Chem., Int. Ed.* **2002**, *41*, 3873.
- (15) Bart, S. C.; Chlopek, K.; Bill, E.; Bouwkamp, M. W.; Lobkovsky, E.; Neese, F.; Wieghardt, K.; Chirik, P. J. *J. Am. Chem. Soc.* **2006**, *128*, 13901.
- (16) Ingleson, M. J.; Pink, M.; Huffman, J. C.; Fan, H.; Caulton, K. G. *Organometallics* **2006**, *25*, 1112.
- (17) Walstrom, A.; Pink, M.; Tsvetkov, N. P.; Fan, H.; Ingleson, M.; Caulton, K. G. *J. Am. Chem. Soc.* **2005**, *127*, 16780.
- (18) Ingleson, M. J.; Yang, X.; Pink, M.; Caulton, K. G. *J. Am. Chem. Soc.* **2005**, *127*, 10846.
- (19) Bourget-Merle, L.; Lappert, M. F.; Severn, J. R. *Chem. Rev.* **2002**, *102*, 3031.
- (20) Ozerov, O. V.; Guo, C.; Fan, L.; Foxman, B. M. *Organometallics* **2004**, *23*, 5573.
- (21) Ozerov, O. V.; Guo, C.; Foxman, B. M. *J. Organomet. Chem.* **2006**, *691*, 4802.
- (22) Ingleson, M. J.; Pink, M.; Caulton, K. G. *J. Am. Chem. Soc.* **2006**, *128*, 4248.
- (23) Ingleson, M.; Fan, H.; Pink, M.; Tomaszewski, J.; Caulton, K. G. *J. Am. Chem. Soc.* **2006**, *128*, 1804.
- (24) El-Ayaan, U.; Murata, F.; Fukuda, Y. *Monatsh. Chem.* **2001**, *132*, 1279.
- (25) Bhadbhade, M. M.; Srinivas, D. *Inorg. Chem.* **1993**, *32*, 6122.
- (26) Heinze, K.; Huttner, G.; Zsolnai, L. *Chem. Ber./Recl.* **1997**, *130*, 1393.
- (27) Fryzuk, M. D.; MacNeil, P. A.; Rettig, S. J.; Secco, A. S.; Trotter, J. *Organometallics* **1982**, *1*, 918.

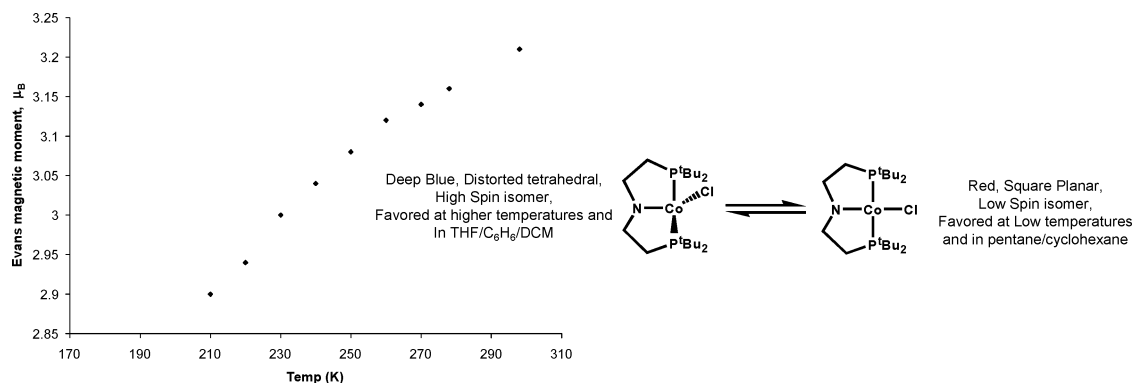


Figure 2. Graphical representation of the variation of solution magnetic moment with temperature for **1**.

ment (angles around cobalt equal 360°), indicating that spin crossover is the origin of the two observed species/colors. Structurally characterized square planar complexes of $\text{Co}^{\text{II}}-\text{Cl}$ are rare, generally requiring stronger field ligands. A Cambridge Structural Database search revealed only one other square planar $\text{Co}(\text{II})$ complex with terminal chlorides, $[\text{Co}_2\text{Cl}_2(\text{C}_8\text{H}_4\text{O}_4)(\text{C}_{12}\text{H}_8\text{N}_2)_2]$, which is geometrically very similar to **1**.²⁸ The only major point of note in the solid-state structure of **1** is the twisting of the Si–N–Si backbone (dihedral angles P1–Co–N–Si1, $28.70(6)^\circ$; P2–Co–N–Si2, $23.80(7)^\circ$) to orient the amide lone pair away from an occupied cobalt d-orbital. Comparison of the structural metrics between the square planar complexes **1** and $^{\text{Ph}}\text{PNPCo}(\text{CH}_2\text{Ph})$ ($^{\text{Ph}}\text{PNP} = [\text{Ph}_2\text{PCH}_2\text{SiMe}_2]_2\text{N}^-$), where the benzyl group is unambiguously η^1 , reveals a number of minor structural differences:²⁹ (i) The Co–P bond distances in **1** (2.2802(4) and 2.2898(4) Å) are longer than those in $^{\text{Ph}}\text{PNPCo}(\text{CH}_2\text{Ph})$ (2.2127 and 2.2162 Å), possibly resulting from the increased steric requirements of the bulkier phosphine ^tBu substituents. The P–Co bond distances are also notably longer in **1** than those in $(\text{PEt}_2\text{Ph})_2\text{Co}(\text{mesityl})_2$ (2.232(4) Å).³⁰ (ii) Compound **1** is significantly closer to the ideal square planar geometry (P–Co–P = $177.41(1)^\circ$ and N–Co–Cl = $178.26(4)^\circ$) than $^{\text{Ph}}\text{PNPCoCH}_2\text{Ph}$ (P–Co–P = $162.93(3)^\circ$, N–Co–C = $173.6(1)^\circ$), although the deformation may be caused by the bulkier benzyl group rather than any specific effects from the change of the PNP ligand. The Co–N distances vary as expected because of the respective ligand field strength of the anionic substituents. Unfortunately, despite repeated attempts under various conditions, crystals of the blue, presumably the high-spin tetrahedral form of PNPCoCl were not obtainable.

Solution studies (298 K, C_6D_6) revealed a compound that, on the NMR time scale, has C_{2v} symmetry (as determined by only three distinct well-defined, paramagnetically shifted, and broadened resonances in ^1H NMR spectrum; Figure 1) and a solution magnetic moment (Evans method) at $3.96 \mu_B$ supporting the high-spin ($S = 3/2$) assignment suggested by the color. In contrast, the solution magnetic moment in C_6D_{12} is $2.85 \mu_B$. This value, while significantly higher than both

the spin-only value ($1.73 \mu_B$) and the values reported²⁹ for the square planar $^{\text{Ph}}\text{PNPCoR}$ series (R = Me, CH_2Ph , $\text{CH}_2\text{-SiMe}_3$; $1.9\text{--}2.2 \mu_B$) is comparable to the solution magnetic moment recorded³¹ for monomeric low-spin $\text{PhB}(\text{CH}_2\text{PPh}_2)_3\text{-CoI}$ ($2.87 \mu_B$). The value of $2.85 \mu_B$ suggests that the low spin form of **1** is, at least, the dominant species in cyclohexane solutions, in sharp contrast to that in C_6H_6 solutions. A comparison of the ^1H NMR spectra of **1** in C_6D_{12} and C_6D_6 (Figure 1) reveals a drastic change in the chemical shifts of the three resonances, with the CH_2 protons (proximal to the paramagnetic cobalt) moving by more than 14 ppm because of the change in solvent; the SiMe_2 and ^tBu resonances shift to a lesser degree. The stepwise addition of an increasing volume of THF to a C_6D_{12} solution of **1** leads to a gradual shift of all the resonances of **1** in the ^1H NMR spectra toward the spectra observed in neat benzene (Figure 1 top), and ultimately, at a volume ratio of 2:1 (THF/ C_6D_{12}), the ^1H NMR spectra is effectively identical to that of **1** in pure THF- d_8 (and it is also blue).

Surprisingly, the solution magnetic moment of **1** in toluene- d_8 ($3.21 \mu_B$) was significantly lower than that found in benzene ($3.96 \mu_B$), implying a higher concentration of the low-spin isomer (the solution magnetic moments were consistent over a number of independently prepared samples). At present, we are unsure why solvents with such similar properties (benzene and toluene) should stabilize different spin states to such a degree. Cooling of a sample of **1** in toluene- d_8 in 10° steps from 298 to 210 K resulted in the expected thermochromism, with a color change from blue to red observed and a gradual decrease in the solution magnetic moment to a minimum of $2.9 \mu_B$ at 210 K (Figure 2). This variation in magnetic moment is fully reversible. The chemical shift of the CH_2 protons (most sensitive to change in metal spin state) over this temperature range travels upfield significantly from the initial position (27.1 ppm at 298 K). At 210 K, the slow-exchange regime is not reached, although the resonances have all broadened dramatically, with the CH_2 resonance is no longer visible. No spin crossover is observed in the solid state: heating of a red powdered sample of **1** in a sealed capillary results in no color change; it decomposes at 110°C to an intractable mixture. It is important to note that the phenyl derivative $^{\text{Ph}}\text{PNPCoCl}$ is rigorously high spin,²⁹ while the ^tBu derivative **1** appears

(28) Xiao, H. P.; Hu, M. L.; Li, X. H. *Acta Crystallogr., Sect. E* **2004**, *E60*, m3336.

(29) Fryzuk, M. D.; Leznoff, D. B.; Thompson, R. C.; Rettig, S. J. *J. Am. Chem. Soc.* **1998**, *120*, 10126.

(30) Falvello, L.; Gerloch, M. *Acta Crystallogr., Sect. B* **1979**, *35*, 2547.

(31) Jenkins, D. M.; Peters, J. C. *J. Am. Chem. Soc.* **2005**, *127*, 7148.

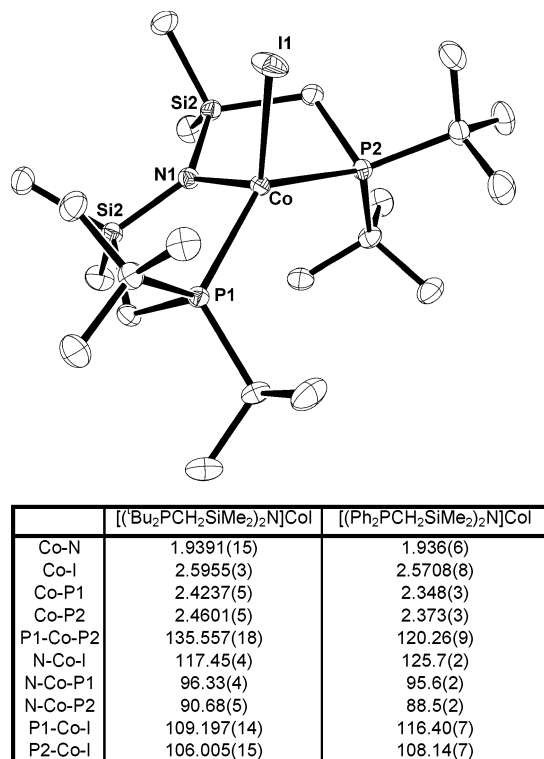


Figure 3. (Above) ORTEP view (50% probabilities) of complex **2**. (Below) Selected bond lengths and angles for **2** and the corresponding values for the related phenyl substituted phosphine complex previously synthesized by Fryzuk et al.

to be on an energetic cusp between high spin and low spin, with subtle solvent changes (benzene to toluene) sufficient to significantly perturb the equilibrium position.

DFT calculations, using the continuum solvent model, show that the two spin states are very similar in free energy. While the low-spin state is favored (ΔG°) by 4.9 kcal/mol in the gas phase or by 4.0 kcal/mol in cyclohexane, this decreases to 2.9 kcal/mol in THF (still favoring low spin).

In an attempt to produce crystalline material analogous to high-spin **1** that may afford insight into the contrasting behavior of **1** compared to its phenyl derivative, PNPCoI, **2** was synthesized in reasonable yield as a turquoise crystalline solid. Isolated yields for **2** (and other PNP ligated complexes) are consistently lower than optimal because of the extremely high solubility imparted by the lipophilic PNP ligand. An X-ray diffraction study revealed (Figure 3) monomeric PNPCoI, with an environment around cobalt significantly distorted from ideal tetrahedral toward a cis-divacant octahedron (Figure 3). The bond lengths to cobalt are consistently longer in **2** than in **1**, as expected with the change in spin state. The structural characterization of **2** allows for an examination into the effect that the change of the phosphine substituent on the PNP ligand has on the solid-state structure by comparison with the previously determined²⁹ structure of ^{Ph}PNPCoI. Upon inspection, there are three significant differences: (i) The Co–P bond lengths in **2** are significantly longer than that for the phenyl derivative. (ii) The P–Co–P angle in **2** is larger (by $\sim 15^\circ$). (iii) The N–Co–I angle in complex **2** is smaller (by 8.3°). The first two effects are a direct result of the increased steric bulk generated by the

four ^tBu groups, with the structural differences reducing the larger steric repulsion between ^tBu groups. The assumption of a similar structure for high-spin **1** leads to the conclusion that the increased stability of the low-spin isomer observed for **1** compared to that of ^{Ph}PNPCoCl is dominated by the distal phosphine steric bulk, with the square planar structure stabilized because it enables a strict *trans*-phosphine disposition, thereby minimizing the steric repulsion between ^tBu groups (corroborated by the significantly smaller minimum C–C contact observed between ^tBu carbons of “*trans*”-disposed phosphines in high-spin **2** (3.785 Å) compared to that in low-spin **1** (4.545 Å)). This effect more than offsets the contraction of the P–Co bonds inherent in moving from high-spin Co(II) to low-spin Co(II). The effects of the increased steric pressure present in **2** (and by inference in the high-spin isomer of **1**) may also prevent the high-spin structure from approaching the minimum energy conformation around cobalt, in comparison to the sterically unhindered phenyl derivative, resulting in a higher-energy quartet state. An electronic effect caused by the presence of the stronger σ -donor alkyl phosphine in **1** may also contribute to stabilization of the square planar isomer, with an increased orbital splitting arising from the stronger-field phosphine ligand (analogous to square planar (PCy₃)₂NiCl₂ and tetrahedral (PPh₃)₂NiCl₂).⁵

The solution magnetic moment at 298 K for **2** is unambiguously high spin in both C₆D₆ (4.54 μ_B) and C₆D₁₂ (5.05 μ_B); furthermore, cooling of a toluene-d₈ solution of **2** resulted in no observable thermochromism. The magnetic moments of **2** compare closely to other high-spin Co(II) complexes previously reported, for example, Tp^{''}CoI (5.0 μ_B , where Tp^{''} = tris(3-*i*Pr, 5Me pyrazolyl)borate)³² and PhB-(CH₂S^tBu)₃CoCl (4.5 μ_B).² Therefore, substitution of the chloride in **1** for the weaker-field iodide ligand destabilizes the low-spin form enough for it to be no longer detectably populated. Furthermore, the solution magnetic moments for PNPCoI in C₆D₆ (and in C₆D₁₂) are consistently higher than that for PNPCoCl, in contrast to the ^{Ph}PNP ligated series, ^{Ph}PNPCoX (X = Cl, Br, and I), where the solution magnetic moments are all within $4.2 \pm 0.1 \mu_B$,²⁹ this implies that there is a non-negligible amount of the low-spin **1** present upon dissolution in C₆D₆/THF and is consistent with the crystallization of low-spin **1** from THF solutions.

(PNP)Co(N₃). It seemed prudent for comparison purposes (especially of solution magnetic moments) to synthesize a related complex that was exclusively low spin.³³ This was achieved by the reaction of **1** with 10 equiv of NaN₃, which resulted in a color change from deep blue to terracotta, after the mixture was stirred overnight in THF, consistent with a Co^{II} spin change from high spin to low spin. PNPCoN₃, **3**, was isolated in reasonable yield as a microcrystalline red powder that possessed time-averaged C_{2v} symmetry and a solution magnetic moment of 2.47 μ_B (C₆D₆, 298 K). Solutions of **3** behave as strictly low spin, independent of

(32) Reinaud, O. M.; Rheingold, A. L.; Theopold, K. H. *Inorg. Chem.* **1994**, *33*, 2306.

(33) Rheingold, A. L.; Liable-Sands, L. M.; Golan, J. A.; Trofimenko, S. *Eur. J. Inorg. Chem.* **2003**, 2767.

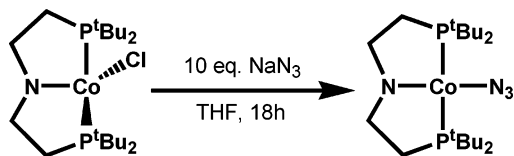


Figure 4. Synthesis of low-spin PNP CoN_3 (**3**) from complex **1** by addition of excess NaN_3 .

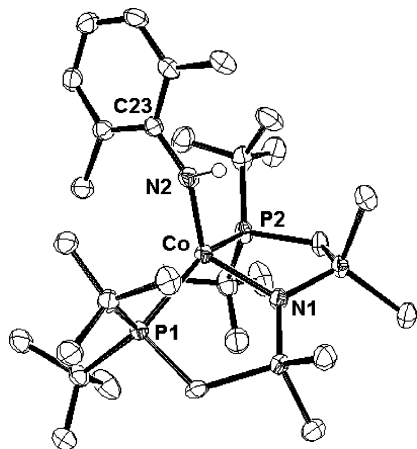


Figure 5. ORTEP view (50% probabilities) of complex **4** (most hydrogens are omitted for clarity). Selected bond lengths (\AA) and angles (deg): Co–N1 = 1.995(2), Co–N2 = 1.916(2), Co–P1 = 2.4966(9), Co–P2 = 2.5209(10), P1–Co–P2 = 141.61(3), N1–Co–N2 = 119.46(10), Co–N2–C23 = 139.6(2), N1–Co–P1 = 91.84(7), N2–Co–P1 = 106.44(8)

solvent and temperature (to 80 °C). The solution magnetic moment of **3** at 2.47 μ_{B} , while still greater than the spin-only value (a common occurrence for low-spin Co(II) compounds), is consistent with the presence of only low-spin **3**. Comparison to the value for **1** in C_6D_{12} (2.85 μ_{B}), suggests that cyclohexane solutions of **1** are only predominated by low-spin **1**; the amount of high-spin isomer is non-negligible. Attempts to produce **3** from the reaction of **1** and stoichiometric or excess TMSiN_3 (TMS = trimethylsilyl) in benzene failed, with **1** recovered unreacted.

(PNP) $\text{Co}[\text{NH}(2,6\text{-Me}_2\text{-C}_6\text{H}_3)]$. It was also of interest to examine the effect that the substitution of halide in **1** for a more sterically demanding, yet weaker ligand field (i.e., a high-spin directing ligand), anionic ligand would have on the resultant structure. Would sterics or electronics dominate the energetics of the structure? The amido complex, PNP $\text{CoN}(\text{H})\text{-}2,6\text{-Me}_2\text{-C}_6\text{H}_3$, **4**, is synthesized by reaction of **1** with a stoichiometric equivalent of $\text{LiN}(\text{H})\text{-}2,6\text{-Me}_2\text{-C}_6\text{H}_3$ in THF, with a rapid color change from deep blue to purple observed. Standard workup and recrystallization from minimum pentane at -40 °C allowed for unambiguous characterization as the high-spin isomer (Figure 5). The gross structure around cobalt is comparable for complexes **2** and **4**, implying similar electronic structures; this is supported by the observed high-spin solution magnetic moment (4.28 μ_{B} , 298 K, Evans method). There are a number of subtle changes in the ligand geometry that act to reduce the steric impact between the amido *ortho*-methyls and ligand *t*butyl groups: (1) An increase in the P–Co–P angle in **4** (141.61(3)°) compared to **2** (135.557(18)°) to increase interphosphine spacing. (2) The Co–N2–C23 angle (139.6(2)°) is greater than systems^{34–36} with low steric crowding (angles in the

range of 123–130°), thereby increasing amido *ortho*-methyl-phosphine *t*Bu separation. (3) The P–Co bonds in **4** (Co–P1, 2.4966(9) \AA ; Co–P2, 2.5209(10) \AA) are longer than those in **2** (Co–P1, 2.4237(5) \AA ; Co–P2, 2.4601(5) \AA). Thus the PNP ligand has some degree of flexibility and can undergo minor structural rearrangements, as opposed to spin isomerism, to reduce steric crowding.³⁷ The final noteworthy point is from comparison of the two Co–amido distances in **4**, which reveals a slightly longer PNP backbone Co–N distance; this we attribute to the constraint inherent in the two fused five-membered rings of the PNP ligand rather than any multiple bonding between Co–N2 (further supported by the effectively identical distances of Co–N2 in **4** (1.916(2) \AA) and Co–N1 in **2** (1.9391(5) \AA)).

The ^1H NMR of complex **4** reveals solution C_{2v} symmetry and displays isotropically shifted resonances for SiMe, *t*Bu, CH_2 , and phenyl *ortho*-methyls; despite numerous attempts, the resonance for the phenyl protons and N–H were not detectable. Furthermore, the N–H stretch was not observable in the infrared spectrum. The similarity of the solid-state structure of **4** to that found for complex **2** confirms its identity as a Co(II) amido complex, with a possible Co(III) imido complex expected to have a significantly different structure and magnetic moment. It is also noteworthy that despite the reducing ability of lithium amides, there is no evidence for any cobalt reduction, with salt metathesis the only reaction observed here.

With the full characterization and elucidation of the solution behavior of these basic PNP CoX complexes in hand, their chemistry was explored.

Oxidation Reactions of PNP CoX . Formation of P(O)–NP(O)CoX. Compounds **1**, **2**, and **3** all proved to be highly oxygen sensitive (and to a lesser degree moisture sensitive).^{38–40} The addition of dry O_2 to a degassed benzene solution of **1** resulted in an immediate color change from deep blue to light blue. Inspection of the ^1H NMR spectrum revealed complete consumption of **1** and the appearance of six new paramagnetic signals that, by their relative intensities (18:18:6:6:2:2), can be assigned to a single new C_s symmetric product. It is noteworthy that nonplanar (PNP) CoX compounds show apparent C_{2v} symmetry because of the rapid (at 25 °C) achievement of a planar structure in a fluxional process. In [P(O)NP(O)] CoX species, any such inversion has a higher barrier because all diastereotopic substituents show separate signals at 25 °C. This is attributed to the larger ring size, making nonplanar structures much more favorable than planar structures. Mass spectroscopy confirmed the addition of two atoms of oxygen, while the solution magnetic moment (4.50 μ_{B}) supported the presence of three unpaired electrons,

(34) Brown, S. D.; Peters, J. C. *J. Am. Chem. Soc.* **2004**, *126*, 4538.

(35) Cowan, R. L.; Trogler, W. C. *J. Am. Chem. Soc.* **1989**, *111*, 4750.

(36) Villanueva, L. A.; Abboud, K. A.; Boncella, J. M. *Organometallics* **1994**, *13*, 3921.

(37) Hope, H.; Olmstead, M. M.; Murray, B. D.; Power, P. P. *J. Am. Chem. Soc.* **1985**, *107*, 712.

(38) Hu, X.; Castro-Rodriguez, I.; Meyer, K. J. *J. Am. Chem. Soc.* **2004**, *126*, 13464.

(39) Egan, J. W., Jr.; Haggerty, B. S.; Rheingold, A. L.; Sendlinger, S. C.; Theopold, K. H. *J. Am. Chem. Soc.* **1990**, *112*, 2445.

(40) Betley, T. A.; Peters, J. C. *Inorg. Chem.* **2003**, *42*, 5074.

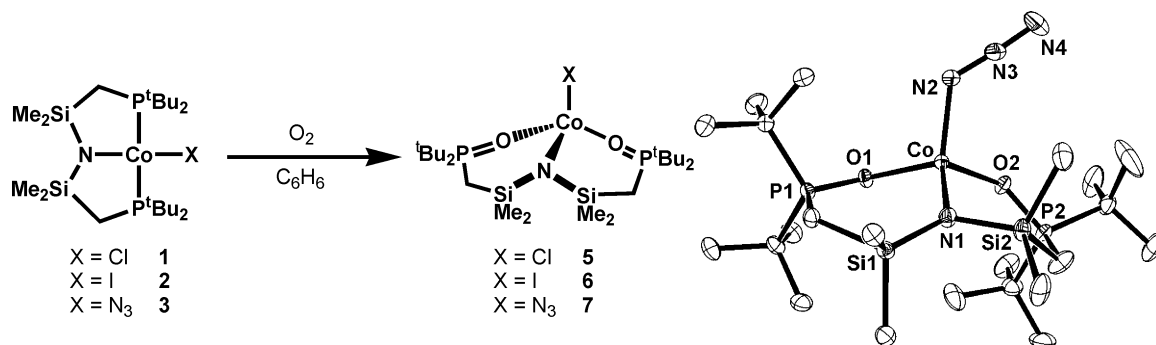


Figure 6. (Left) Synthesis of compounds 5–7 by action of O₂ on precursors 1–3. (Right) ORTEP view (50% probabilities) of one of the molecules of complex 7 found in the asymmetric unit (hydrogens are omitted for clarity). Selected bond lengths (Å) and angles (deg): Co–N1 = 1.981(2), Co–N2 = 1.979(2), Co–O1 = 1.9797(18), Co–O2 = 1.9906(18), P1–O1 = 1.5144(18), N2–N3 = 1.196(3), N3–N4 = 1.161(3), O1–Co–O2 = 109.01(8), N1–Co–O1 = 104.53(8), N1–Co–N2 = 127.50(10), Co–N2–N3 = 125.5(2), N2–N3–N4 = 176.5(3).

consistent with a high-spin, $S = 3/2$ Co(II) center. This leads to a product assignment where the PNP ligand has undergone a four-electron oxidation to give $(^t\text{Bu}_2\text{P}(=\text{O})\text{CH}_2\text{SiMe}_2)_2\text{NCoCl}$, **5** (Figure 6). Analogous reactivity was observed for **2** and **3** to yield $(^t\text{Bu}_2\text{P}(=\text{O})\text{CH}_2\text{SiMe}_2)_2\text{NCoI}$, **6**, and $(^t\text{Bu}_2\text{P}(=\text{O})\text{CH}_2\text{SiMe}_2)_2\text{NCoN}_3$, **7**, respectively. Single crystals suitable for an X-ray diffraction study were obtained by the slow evaporation of a benzene solution of **7** and confirmed a Co(II) tetrahedral complex with both phosphines oxidized. The asymmetric unit contains two independent molecules of **7** that are effectively identical; the structural metrics of only one will be discussed here. The greater flexibility of the two fused six-membered rings (vs five in **3**), combined with the weaker ligand field experienced by cobalt in **7**, allows for a geometry around cobalt closely approaching ideal tetrahedral, considerably more so than that observed in **2** ($\text{O1–Co–O2} = 109.01(8)^\circ$ in **7** compared to $\text{P1–Co–P2} = 135.557(18)^\circ$ in **2**); the only significant deviation from ideal tetrahedral geometry is in the N1–Co–N2 angle, $127.50(10)^\circ$. The Co–N(azide) bond in **7** is elongated ($\text{Co–N2} = 1.979(2)$ Å) compared to those of the other structurally characterized four-coordinate cobalt(II) azide complexes, Tp^*CoN_3 ($\text{Co–N} = 1.911(2)$ Å)³³ and $[(\text{TIMEN})\text{CoN}_3][\text{BPh}_4]$ ⁴¹ ($\text{Co–N} = 1.938(2)$ Å). The remaining bond distances and angles are unremarkable when compared to other tridentate phosphine-oxide cobalt(II) complexes.

In an attempt to observe any intermediates in the reaction between **1** and O₂, the reagents were combined in toluene-*d*₈ at -78 °C, resulting in an immediate reaction (judged by a rapid color change). The ¹H NMR even at this low temperature showed complete consumption of **1**, with only resonances attributable to **5** visible. Complex **5** can alternatively be synthesized quantitatively (by ¹H NMR) from **1** by the addition of 2 equiv of iodobenzene ($\text{PhI}=\text{O}$), producing iodobenzene as a byproduct (by ¹H NMR). Complex **1** however does not react with N₂O (18 h, 25 °C). Complexes **5–7** undergo no reaction upon standing under an atmosphere of dry O₂ for 24 h. Therefore O₂ is not a strong enough oxidant to oxidize cobalt(II) in **5–7**.

Oxidation of PNPCoX with R-X and I₂. Following the work of Fryzuk et al., where ^{Ph}PNPCo(II) halides are successfully oxidized to ^{Ph}PNPCo(III) dihalides by the action

of benzyl halides,¹⁷ we investigated the reactivity of **1** toward benzyl halides. No reaction was observed between **1** and stoichiometric or excess PhCH_2X ($\text{X} = \text{Cl}$ or Br), even after prolonged periods (96 h) or at raised temperatures (18 h at 60 °C), with both **1** and benzyl halide recovered unreacted. This lack of reactivity is in sharp contrast to the phenyl derivative and is paradoxical with the convention that the superior σ -donor phosphine present in **1** would be able to better stabilize the higher oxidation state of Co^{III}. The difference in the observed reactivity might be attributable to distinct ground spin states in the respective Co^{III} products because disparate ground-state electronic structures are found for the cobalt(II) chloride starting materials. It is doubtful that the negative result is caused by the enhanced steric shielding provided upon moving from phenyl to ^tBu substituents on the phosphine, as will be demonstrated later where reactivity occurs with equally bulky reagents. An equally counterintuitive trend was observed by Peters et al.³¹ for the oxidation potentials of Co^{II} in $\text{PhB}(\text{CH}_2\text{PR}_2)_3\text{CoI}$ ($\text{R} = \text{Ph}$ or ⁱPr): the less electron-donating phenyl derivative proved to be significantly easier to oxidize than the more electron-rich ⁱPr analogue.

Despite the above, chloride **1** rapidly reacted with 1 equiv of I₂ in benzene to give a number of new paramagnetic compounds (by ¹H NMR). Suspecting that the multiple products observed would be in part caused by mixed halide isomers, we attempted the reaction between **2** and I₂. This produced one new paramagnetic product with C_s symmetry on the NMR time scale. This complex proved to be only sparingly soluble in benzene, with light blue crystals spontaneously precipitating out of the synthetic solution. An X-ray diffraction study revealed the unanticipated formation of a zwitterionic, tetrahedral, four-coordinate Co^{II} complex, $[\kappa^2-(^t\text{Bu}_2\text{P}(\text{I})\text{CH}_2\text{SiMe}_2\text{NSiMe}_2\text{CH}_2\text{P}^+\text{Bu}_2)\text{CoI}_2]$, **8** (Figure 7). In **8**, one phosphine has been oxidized to a phosphonium cation and is no longer coordinated to cobalt; the resultant cobalt coordination sphere is now occupied by one phosphine, one amide, and two iodides, carrying an overall negative charge to balance the phosphonium cation. Therefore, I₂ has successfully oxidized **2**, but the locus of oxidation is at phosphorus, not cobalt. In **2**, therefore, phosphorus is

(41) Hu, X.; Meyer, K. *J. Am. Chem. Soc.* **2004**, *126*, 16322.

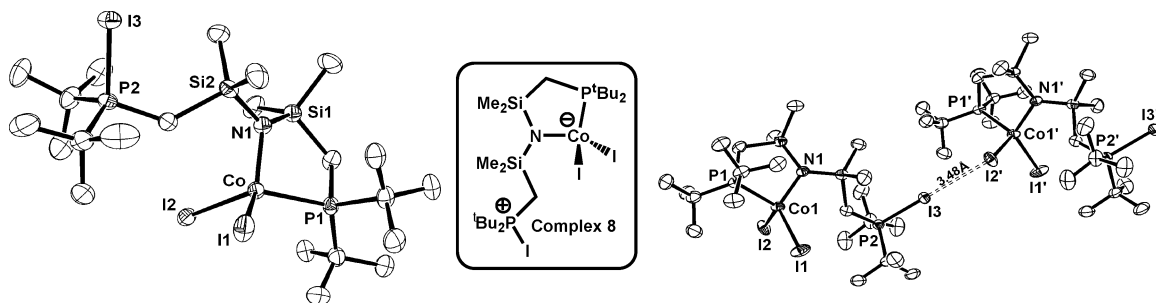


Figure 7. (Left) ORTEP view of complex **8** (hydrogens and a disordered solvent molecule omitted for clarity). (Right) The intermolecular I \cdots I interaction between I3 and I2'. Selected bond lengths (Å) and angles (deg): N1–Co = 1.957(4), Co–I1 = 2.5973(9), Co–I2 = 2.6279(9), Co–P1 = 2.3594(14), P2–I3 = 2.4178(14), I3–I2 = 3.48, P1–Co–N1 = 94.34(14), I1–Co–P1 = 112.32(5), I1–Co–I2 = 107.25(3), I2–Co–N1 = 109.56(13).

more reducing than Co^{II}. This divergence in phosphine reactivity compared to that of the phenyl derivative is clearly caused by the electron-rich ^tBu substituents making the phosphorus in **1** (and **2**) significantly more reducing. The structural metrics of **8** are unremarkable, with the geometry around cobalt close to ideal tetrahedral with only minor distortions arising from the constraints of the remaining five-membered ring. The only observed anomaly is an elongation of the Co–I2 bond (Co–I1, 2.5973(9) Å; Co–I2, 2.6279(9) Å), further highlighted by comparison to the Co–I bond length in **2** (2.5955(3) Å). The source of this becomes clear on examination of the extended structure of **8**, which reveals a close PI \cdots ICo intermolecular contact which, at 3.48 Å, is within the combined van der Waals radii of two iodines. This interaction propagates complex **8** into a one-dimensional polymer in the solid state (Figure 7). Similar I \cdots I interactions are well documented⁴² and arise from the different formal charges associated with each iodine, with I3 formally positively charged, while the I2 bonded to the d⁷ center is unambiguously δ^- .

NMR studies in THF-*d*₈ (in which **8** is significantly more soluble) confirms the expected high-spin nature of **8** with a solution magnetic moment of 4.7 μ_B , corresponding to a Co(II) center with three unpaired electrons ($S = 3/2$). Furthermore a ³¹P{¹H} resonance for the oxidized phosphine, not coordinated to cobalt, is observed as a broadened singlet at +269 ppm; the larger than expected downfield shift is caused by the long-range paramagnetic influence of the high-spin cobalt. At no stage is a five-coordinate trivalent PNPCoI₂ complex, analogous to the fully characterized ^{Ph}PNPCoX₂ (X = Cl, Br),¹⁷ observed. Complex **8** is indeed one of the products observed (by ¹H and ³¹P{¹H} NMR spectroscopy) in the reaction mixture generated by **1** and I₂, confirming that a similar phosphine oxidation has occurred.

The addition of 1 equiv of I₂ to complex **8** in THF-*d*₈ produces a single new paramagnetic C_{2v} symmetric product that within minutes proceeds to precipitate out as a microcrystalline green powder. The lack of solubility in suitable solvents has frustrated further identification of this complex, but it is reasonable to postulate that iodination of the second phosphine has occurred, opening the second five-membered ring, to generate a bis-phosphonium salt (Figure 8), with the poor solubility then attributable to the formation of an

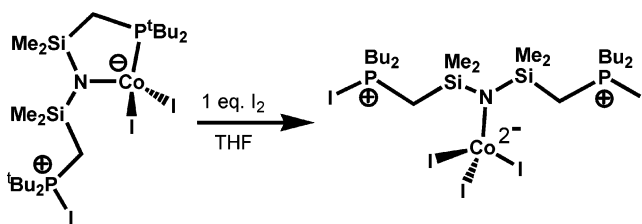


Figure 8. Reaction of complex **8** with a stoichiometric equivalent of I₂, leading to the probable insoluble product [(I-P⁺Bu₂CH₂SiMe₂)₂NCoI₃].

extended structure through extensive intermolecular I^{δ+}...I^{δ-} interactions.

Oxidation of **1** (or **2**) in THF with an outer-sphere oxidant, ferrocenium, Cp₂Fe⁺ (as the PF₆ and BARF salts) also failed, with the starting materials unchanged after 24 h at 20 °C. Oxidation of **1** by reaction with TEMPO or Galvinoxyl free radicals was also unsuccessful, with complex **1** unchanged after 24 h at 25 °C in the presence of a stoichiometric equivalent of either of these reagents. Finally oxidation of **1** was also attempted with stoichiometric AgOTf in THF. This led to a number of new paramagnetic products, along with a diamagnetic “PNPAg” complex (as determined by the ³¹P{¹H} NMR spectra, exhibiting the characteristic two-doublet pattern for coupling of phosphorus to ¹⁰⁷Ag and ¹⁰⁹Ag). This reaction mixture proved to be intractable; furthermore, attempts to produce a single product by use of excess AgOTf were equally unsuccessful. Thus Co(III) halide/pseudo-halide complexes of the PNP ligand would appear to be either totally inaccessible or transient, in contrast to Fryzuk’s ^{Ph}PNP ligated cobalt.²⁹

It was hypothesised that the complex mixture observed above may have arisen from the bifunctionality of the AgOTf reagent, with it able to function via salt metathesis or oxidation pathways. The metathesis reaction was independently investigated using the redox-innocent cations Li⁺, Tl⁺, and Na⁺; all of these triflates failed to react with **1** in THF even after extended periods (3 days). Reaction of **1** with equimolar TMSOTf resulted in the partial conversion to a new paramagnetic product with C_{2v} symmetry in the ¹H NMR spectrum (this product was evident in the reaction between AgOTf and **1**). The yield of this product could be enhanced by the use of a large excess of TMSOTf (~100 equiv), although unreacted **1** still remained.

Recrystallization of a sample of **1** in the presence of 100 equiv of TMSOTf solution yielded two sets of crystals, red crystals of **1** and dark blue crystals of sufficient quality for

(42) McAuliffe, C. A.; Godfrey, S. M.; Mackie, A. G.; Pritchard, R. G. *Angew. Chem.* **1992**, *104*, 932.

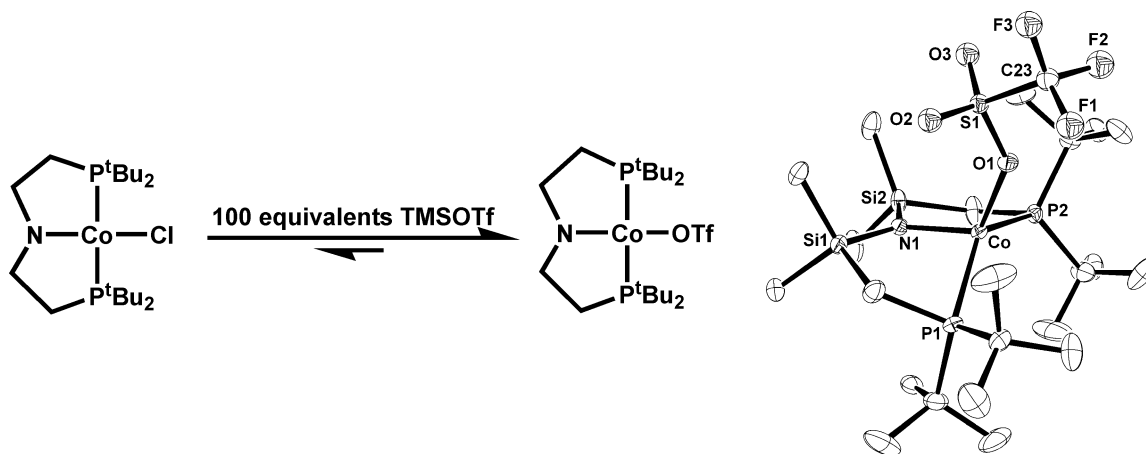


Figure 9. (Left) Equilibrium established between complexes **1** and **9** in the presence of a 100-fold excess of TMSOTf. (Right) ORTEP view (50% probabilities) of complex **9** (only one of the two disordered sites for one 'Bu and the triflate are shown, hydrogens are also omitted for clarity). Selected bond lengths (Å) and angles (deg): Co–N1 = 1.928(3), Co–P1 = 2.4182(10), Co–P2 = 2.3942(10), Co–O1 = 2.035(2), P1–Co–P2 = 135.70(4), P1–Co–N1 = 93.43(9), P2–Co–N1 = 97.94(9), N1–Co–O1 = 118.95(11), P1–Co–O1 = 106.78(8), P2–Co–O1 = 104.60(8).

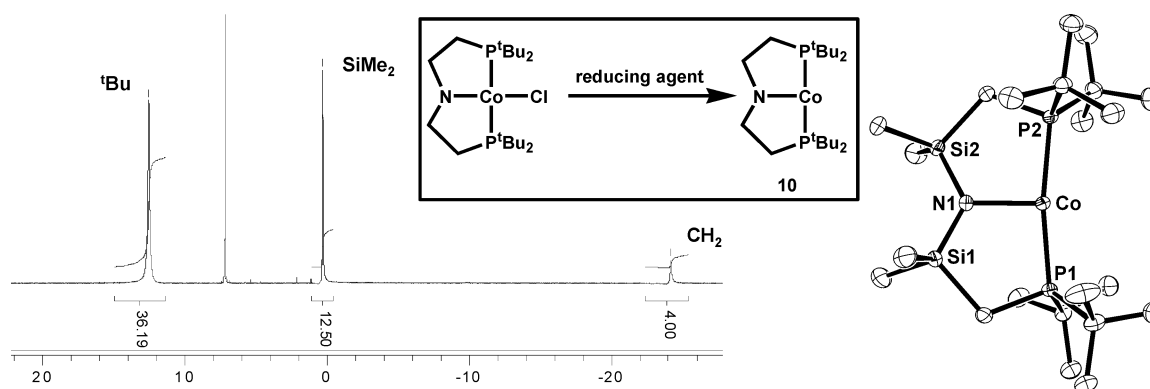


Figure 10. (Left) ^1H NMR (C_6D_6 , 298 K) for complex **10**. (Right) ORTEP view (50% probabilities) of complex **10** (hydrogens are omitted for clarity). Selected bond lengths (Å) and angles (deg): Co–N1 = 1.9735(15), Co–P1, 2.2281(6), Co–P2 = 2.2237(6), P1–Co–P2 = 170.56(2), P1–Co–N1 = 94.65(5), P2–Co–N1 = 94.75(5).

an X-ray diffraction study. This revealed the product to be the anticipated $\text{PNPCo}(\text{OTf})$, **9**. The structure of **9** (Figure 9) is analogous to that observed for **2**, with minimal variation in bond angles (e.g., for complex **9**, $\text{P1–Co–P2} = 135.70(4)^\circ$ and $\text{N–Co–O} = 118.95(11)^\circ$, while for complex **2**, $\text{P1–Co–P2} = 135.557(18)^\circ$ and $\text{N–Co–I} = 117.45(4)^\circ$), precluding any structural distortion caused by the increased steric profile of triflate. The bond lengths to cobalt in **9** exhibit a minor contraction compared to the analogous bonds in **2**, presumably to compensate for the poorer donor ability of triflate. The cobalt–triflate bond length in **9** is considerably longer ($\text{Co–O1} = 2.035(2)$ Å) than that reported⁴³ for another high-spin distorted tetrahedral $\text{Co}^{\text{II}}\text{–OTf}$ complex, $\text{Tp}^{\text{Ph,Me}}\text{Co–OTf}$ ($\text{Co–O} = 1.963(3)$ Å). This relative lengthening is presumably influenced by the superior electron donating properties of the PNP ligand. The excellent solubility of complex **9** in C_6H_6 confirms that the triflate is coordinated to cobalt in this nonpolar environment. The difficulties in obtaining any useful quantities of pure complex **9** frustrated further characterization and any reactivity studies.

Alkylation/Reduction of PNPCoX . Thermally stable four-coordinate cobalt(II) alkyl complexes using other tri-

dentate monoanionic ligands are well documented^{29,44,45} and following the divergence in reactivity observed between **1** and PhPNPCoCl , we next investigated the alkylation of **1** with a variety of alkyl lithiums. The phenyl-substituted phosphine derivative readily forms square-planar Co^{II} alkyl complexes, and we were interested in determining if the better σ -donor alkyl phosphine would allow for the formation of analogous PNPCoR complexes. The addition of stoichiometric MeLi , PhMgCl , or $\text{LiCH}_2\text{SiMe}_3$ to **1** at -78 °C in THF resulted in a rapid color change to green. The ^1H NMR spectra revealed an identical new product from all three reactions, each displaying three new paramagnetically shifted resonances, confirming C_{2v} symmetry. The reagent independence coupled with a significant reduction in the peak width at half-height (Figure 10) observed in the ^1H NMR spectra (compared to Co^{II} $S = 1/2$ and $3/2$ PNPCoX complexes) suggested a different spin state; therefore a redox change at cobalt (the line widths of equivalent groups in paramagnetic complexes is highly dependent on the number of unpaired electrons at the metal center).^{46,47} At no time in the attempted alkylation

(43) Uehara, K.; Hikichi, S.; Akita, M. *J. Chem. Soc., Dalton Trans.* **2002**, 3529.

(44) Jewson, J. D.; Liable-Sands, L. M.; Yap, G. P. A.; Rheingold, A. L.; Theopold, K. H. *Organometallics* **1999**, *18*, 300.

(45) DuPont, J. A.; Coxey, M. B.; Schebler, P. J.; Incarvito, C. D.; Dougherty, W. B.; Yap, G. P. A.; Rheingold, A. L.; Riordan, C. G. *Organometallics* **2007**, *26*, 971.

of **1** are any intermediates observed; thus if a compound PNP CoR is formed, it is extremely short-lived. Attempted alkylations leading to a reduction of a first-row transition metal complex (including those of cobalt) are well precedented,^{48–51} and the observation of an identical ^1H NMR spectrum in the reaction of **1** (or **2**) with excess magnesium powder (or stoichiometric sodium naphthalide) confirmed that reduction of cobalt indeed occurred. The 1:1 reaction stoichiometry suggested a one-electron reduction of cobalt to a d^8 Co^I species, confirmed by a solution magnetic moment measurement (at 298 K, C_6D_6) of $3.2 \mu_{\text{B}}$, consistent with a triplet ($S = 1$) ground state. The deviation above the spin-only value ($2.83 \mu_{\text{B}}$) is common for cobalt complexes (e.g., $\text{TpCo}(\text{C}_2\text{H}_4) = 3.8 \mu_{\text{B}}$ ⁵² and $(\text{TIMEN}^{\text{xy}})\text{Co}^+ = 3.65 \mu_{\text{B}}$)³⁸ and can be attributed to a substantial contribution from the orbital angular momentum of cobalt. An X-ray diffraction study on green crystals formed from cooling a concentrated toluene solution to -40°C overnight revealed the formation of three coordinate PNP Co , **10** (Figure 10), with no agostic or weak donor (e.g., THF or toluene) occupying the fourth site trans to the amide nitrogen.

The geometry around cobalt in complex **10** is planar (angles = 360°) and closely approximates a T-shape, with a slight expansion of the two five-membered rings of **10** ($\text{N1-Co-P1} = 94.65(5)^\circ$ and $\text{N1-Co-P2} = 94.75(5)^\circ$), resulting in an improved encapsulation of the low-coordinate cobalt center (compared to $\text{N1-Co-P1} = 89.46(3)^\circ$ and $\text{N1-Co-P2} = 89.73(3)^\circ$ in **1**). Thus, complex **10** is the analog of the three-coordinate skeletal pincer complex (pincer) M ($\text{M} = \text{Rh}$ or Ir) that has been previously postulated^{53–57} as a intermediate in a number of challenging small molecule activations, but hitherto not observed. Inspection of the bond lengths around cobalt in **10** reveal shortened Co-P bonds and a lengthened N-Co bond (by comparison to **1**); it is difficult to ascribe this to any one factor because it can be attributed to the change in spin state at cobalt, the change in sterics around cobalt on reduction in coordination number and/or the increased electron deficiency at cobalt in **10** (complex **10** is a formally 14-electron compound if we

assume the amide is a one-electron donor). The two SOMOs of (PNP) Co are x_2-y_2 and z_2 .⁵⁸ Three-coordinate cobalt complexes are documented,^{37,59,60} although only in the oxidation states +2 and +3; to the best of our knowledge, complex **9** is the first three-coordinate Co^I complex to be structurally characterized. A number of three-coordinate d^8 Ni complexes are known,^{61–63} and all assume a geometry best described as trigonal planar in contrast to **10**. Two bona fide (i.e., without agostic or other weak donor interactions) three-coordinate d^8 rhodium complexes have been structurally determined,⁶⁴ one⁶⁵ with a nonchelate analog of the PNP ligand, $\text{Rh}(\text{PET}_3)_2[\text{N}(\text{SiMePh}_2)_2]$. Interestingly this nonchelate restrained complex assumes a distorted trigonal planar geometry (angles around rhodium sum to 360°), implying that the T-shaped geometry observed for **10** is not the most stable electronic configuration for a bisphosphine amido ligated group nine metal. Furthermore, the amide plane in $\text{Rh}(\text{PET}_3)_2[\text{N}(\text{SiMePh}_2)_2]$ is orthogonal to the RhP_2 plane, while the constraints of the PNP chelate prevent this conformation in **10**. Care must be taken in this comparison because **10** has a triplet ground state compared to the singlet ground state observed for the 4d metal complex $\text{Rh}(\text{PET}_3)_2[\text{N}(\text{SiMePh}_2)_2]$, and this may have a significant effect because the spin state and geometry are interrelated. The second d^8 three-coordinate complex⁶⁴ (β -diketiminato) RhCOE , assumes a distorted T-shaped geometry analogous to that of **10** and again is diamagnetic, as expected for the second-row rhodium, in contrast to the cobalt center in **10**. Also of note is a three-coordinate Rh pincer complex, $[\text{C}_{10}\text{H}_5(\text{CH}_2\text{P}^i\text{Pr}_2)_2\text{Rh}]^-$, recently reported by Milstein et al.⁶⁶ (not structurally characterized), which although anionic is still $\text{Rh}(I)$ and can be expected to be geometrically identical to complex **10**.

Complex **10** is indefinitely stable in the solid state under inert atmosphere and stable for weeks in solution (even upon heating to 60°C for 24 h in C_6D_6). The stability and the absence of any weak donor coordination in the fourth site of **10** can be attributed to its high-spin nature, with the energy needed to induce spin pairing (to generate a low-lying vacant orbital and bind and subsequently activate a fourth ligand) not recouped by weak donors. It should however be noted that, with the existence of two singlet ground state, three-coordinate, rhodium d^8 complexes, a high-spin metal center is not a prerequisite for the formation of three-coordinate M^I d^8 complexes. The reluctance of **10** to bind weak donors is further highlighted by the lack of formation of any new products upon cooling of a THF- d_8 (or toluene- d_8) solution

- (46) Yu, Y.; Smith, J. M.; Flaschenriem, C. J.; Holland, P. L. *Inorg. Chem.* **2006**, *45*, 5742.
 (47) Lu, C. C.; Saouma, C. T.; Day, M. W.; Peters, J. C. *J. Am. Chem. Soc.* **2007**, *129*, 4.
 (48) Sugiyama, H.; Aharonian, G.; Gambarotta, S.; Yap, G. P. A.; Budzelaar, P. H. M. *J. Am. Chem. Soc.* **2002**, *124*, 12268.
 (49) Kooistra, T. M.; Knijnenburg, Q.; Smits, J. M. M.; Horton, A. D.; Budzelaar, P. H. M.; Gal, A. W. *Angew. Chem., Int. Ed.* **2001**, *40*, 4719.
 (50) Bouwkamp, M. W.; Lobkovsky, E.; Chirik, P. J. *J. Am. Chem. Soc.* **2005**, *127*, 9660.
 (51) Gibson, V. C.; Humphries, M. J.; Tellmann, K. P.; Wass, D. F.; White, A. J. P.; Williams, D. J. *Chem. Commun.* **2001**, 2252.
 (52) Detrich, J. L.; Konecny, R.; Vetter, W. M.; Doren, D.; Rheingold, A. L.; Theopold, K. H. *J. Am. Chem. Soc.* **1996**, *118*, 1703.
 (53) Wang, K.; Goldman, M. E.; Emge, T. J.; Goldman, A. S. *J. Organomet. Chem.* **1996**, *518*, 55.
 (54) Xu, W.-w.; Rosini, G. P.; Krogh-Jespersen, K.; Goldman, A. S.; Gupta, M.; Jensen, C. M.; Kaska, W. C. *Chem. Commun.* **1997**, 2273.
 (55) Gupta, M.; Hagen, C.; Flesher, R. J.; Kaska, W. C.; Jensen, C. M. *Chem. Commun.* **1996**, 2083.
 (56) Zhu, K.; Achord, P. D.; Zhang, X.; Krogh-Jespersen, K.; Goldman, A. S. *J. Am. Chem. Soc.* **2004**, *126*, 13044.
 (57) Liu, F.; Pak, E. B.; Singh, B.; Jensen, C. M.; Goldman, A. S. *J. Am. Chem. Soc.* **1999**, *121*, 4086.

- (58) See Supporting Information.
 (59) Dai, X.; Kapoor, P.; Warren, T. H. *J. Am. Chem. Soc.* **2004**, *126*, 4798.
 (60) Holland, P. L.; Cundari, T. R.; Perez, L. L.; Eckert, N. A.; Lachicotte, R. J. *J. Am. Chem. Soc.* **2002**, *124*, 14416.
 (61) Eckert, N. A.; Bones, E. M.; Lachicotte, R. J.; Holland, P. L. *Inorg. Chem.* **2003**, *42*, 1720.
 (62) Campora, J.; Reyes, M. L.; Mereiter, K. *Organometallics* **2002**, *21*, 1014.
 (63) Kogut, E.; Wiencko, H. L.; Zhang, L.; Cordeau, D. E.; Warren, T. H. *J. Am. Chem. Soc.* **2005**, *127*, 11248.
 (64) Budzelaar, P. H. M.; De Gelder, R.; Gal, A. W. *Organometallics* **1998**, *17*, 4121.
 (65) Zhao, P.; Krug, C.; Hartwig, J. F. *J. Am. Chem. Soc.* **2005**, *127*, 12066.
 (66) Frech, C. M.; Ben-David, Y.; Weiner, L.; Milstein, D. *J. Am. Chem. Soc.* **2006**, *128*, 7128.

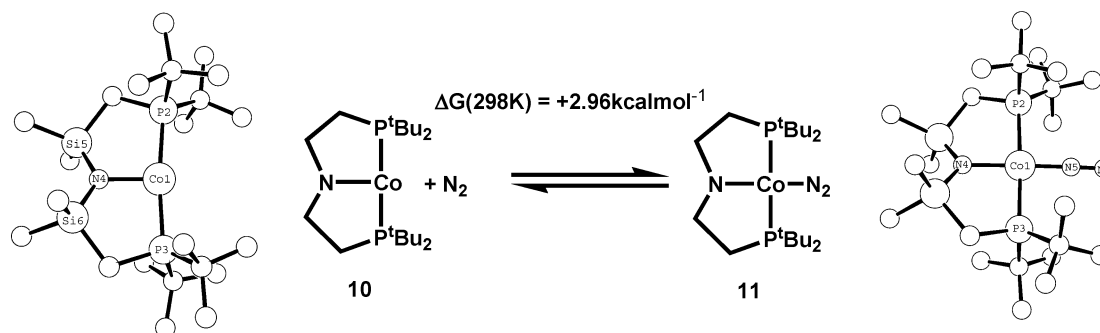


Figure 11. (Left) DFT geometry optimized structure for complex **10**. (Center) Essentially thermoneutral binding of N_2 to $PNPCo$ at 298 K. (Right) DFT geometry optimized structure for singlet ($S = 0$), $PNPCo(N_2)$, **11**. Selected bond lengths (\AA) and angles (deg) for the calculated structure of **11**: $Co1-P2 = 2.29$, $Co1-P3 = 2.29$, $Co-N4 = 1.94$, $Co1-N5 = 1.72$, $N5-N6 = 1.15$, $P2-Co1-P3 = 176.4$, $P2-Co1-N4 = 88.9$, $P2-Co1-N5 = 91.3$, $N4-Co1-N5 = 115.3$.

to $-70\text{ }^\circ\text{C}$ (by ^1H NMR); at no point are any diamagnetic products (i.e., $PNPCo(\text{solvent})$) observed. The distal steric bulk of the phosphine ^tBu groups, in addition to enforcing the unusual planar T-shaped geometry, prevent the dimerization observed for a closely related PNP ligand [$(i\text{Pr}_2\text{P}(m\text{-C}_6\text{H}_4)_2\text{N})^-$ that forms a dimer with an anilido bridged $[\text{Co}_2\text{N}_2]$ core.⁶⁷

Again the performance of a simple reaction (alkylation of a metal halide) has resulted in a distinct outcome for the ^tBu derivative of the PNP ligand compared to the phenyl derivative. A possible explanation, based on the observed product **10**, is that the replacement of halide by a strong σ -donor ligand (alkyl/aryl) would result in a metal center that is extremely electron-rich (overloaded) and thus prone to undergo reduction by a formal Co-R bond homolysis. The success of Fryzuk et al. in synthesising $^{\text{Ph}}\text{PNPCoR}$ is then attributed to the presence of poorer donor bis-aryl phosphines and consequently a less electron-rich metal center. A similar trend (i.e., an increased ease of metal reduction on phenyl for alkyl exchange on phosphine substituent) to that hypothesized here, has been observed in the Fe(II) complexes, $\text{PhB}(\text{CH}_2\text{PR}_2)_3\text{FeCl}$ ($\text{R} = \text{Ph}$ and ^iPr).⁷⁹

Binding of Neutral Two Electron Donors to Complex 10. The reluctance of complex **10** to bind weak donor solvents (even at low temperature) led us to probe the reactivity of **10** with respect to small neutral two-electron donors.

(a) N_2 . The charging of a degassed toluene solution of **10** with 1 atm of N_2 resulted in no observable color change and a ^1H NMR spectrum consistent with the presence of only **10**. However, the infrared spectrum in a N_2 -saturated pentane solution revealed one low-intensity peak in the expected range for $\nu(N_2)$ (2004 cm^{-1}). This observation implied the presence of a low concentration of a coordinated dinitrogen complex. This was confirmed by a low-temperature NMR study in toluene- d_8 , which at temperatures below $-10\text{ }^\circ\text{C}$, revealed the growth of a new diamagnetic C_{2v} product. When it reached $-50\text{ }^\circ\text{C}$, the solution was a terracotta color, and the diamagnetic product had increased in concentration (**10** is still observed, although now the minor constituent). A $^{31}\text{P}\{-^1\text{H}\}$ NMR resonance was observed as a broad singlet at

66.3 ppm along with a ^1H NMR spectrum displaying ligand resonances in the expected diamagnetic region. Returning the solution to $25\text{ }^\circ\text{C}$ produced a NMR spectrum displaying only resonances attributable to **10**. Repeating the low-temperature NMR study under an argon atmosphere resulted in no observable diamagnetic products at $-50\text{ }^\circ\text{C}$, verifying that the new diamagnetic product is a dinitrogen compound of $PNPCo$. The time-averaged C_{2v} symmetry combined with the single $\text{N}\equiv\text{N}$ stretching frequency attests to a monoadduct, presumably $PNPCo(N_2)$, **11**. A dinitrogen bridged complex $(\text{PNP})\text{Co-N}\equiv\text{N-Co}(\text{PNP})$ is an alternative (as previously reported⁶⁷ with a related, albeit sterically more compact, PNP ligand); we disfavor this possibility because of the extreme steric crowding associated with the ^tBu phosphine substituents and on the basis of DFT calculations (see below). We would expect such a bridged dinitrogen complex to have a weak or even symmetry-forbidden N/N stretch. There is no evidence for the coordination of a second molecule of N_2 . Complex **10** therefore reversibly binds N_2 to generate **11**, an equilibrium that favors **10** at room temperature, but upon cooling (thereby reducing the entropic penalty), complex **11** dominates. Comparison of the $\text{N}\equiv\text{N}$ stretch for **11** (2004 cm^{-1}) with other four-coordinate Co^I dinitrogen complexes (e.g., pseudotetrahedral Tp^+CoN_2 , 2046 cm^{-1})⁵² exemplifies the strong effect of the amide π -donor.

To probe the energetics of this conversion (which has to be essentially thermoneutral, i.e., $\Delta G = 0 \pm 3\text{ kcalmol}^{-1}$), DFT calculations were performed on complexes **10** and **11** and on the energy profile of their interconversion (Figure 11). The computation proved to be extremely density-functional-dependent, as previously found by Harvey and co-workers^{68–70} for other 3d metal systems, with the widely used hybrid functionals that include “exact” exchange leading to an artificially more stable high-spin state. As a result, pure nonlocal functionals are a better choice for our reactions involving a change in spin state. The choice of functional for all our DFT studies of $(\text{PNP})\text{CoL}_n$ was calibrated by its ability to successfully predict the equilibrium of $(\text{PNP})\text{Co}(\text{triplet}) + N_2 \rightarrow (\text{PNP})\text{Co}(N_2)$ (singlet) (to agree with the

(68) Harvey, J. N. *Struct. Bonding (Berlin, Germany)* **2004**, *112*, 151.

(69) Carreon-Macedo, J.-L.; Harvey, J. N. *J. Am. Chem. Soc.* **2004**, *126*, 5789.

(70) Broenstrup, M.; Schroeder, D.; Kretzschmar, I.; Schwarz, H.; Harvey, J. N. *J. Am. Chem. Soc.* **2001**, *123*, 142.

(67) Fout, A. R.; Basuli, F.; Fan, H.; Tomaszewski, J.; Huffman, J. C.; Baik, M.-H.; Mindiola, D. J. *Angew. Chem., Int. Ed.* **2006**, *45*, 3291.

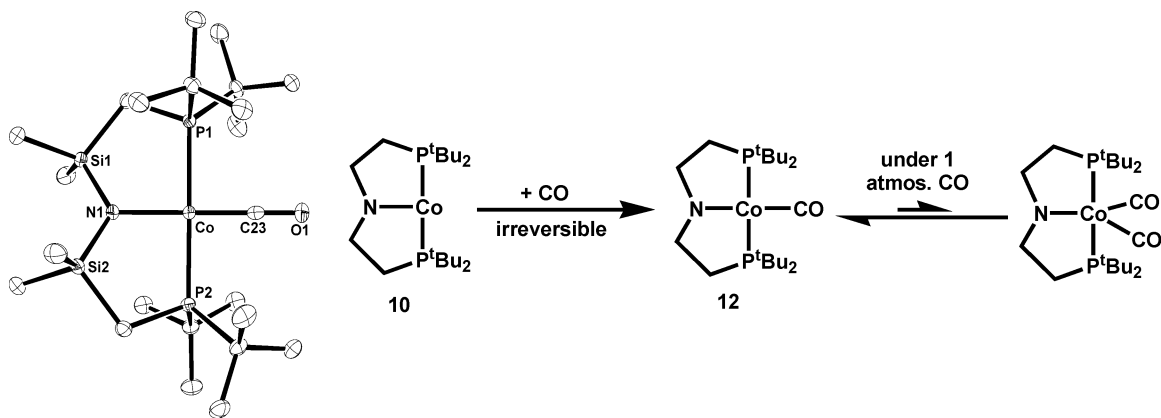


Figure 12. (Left) ORTEP view (50% probabilities, hydrogens omitted for clarity) of complex **12**. (Right) Equilibrium between the mono- and dicarbonyl complexes under 1 atm of CO. Selected bond lengths (Å) and angles (deg) for **12**: N1–Co = 1.9478(15), P1–Co = 2.2322(5), P2–Co = 2.2348(5), Co–C23 = 1.692(2), C23–O1 = 1.167(3), P1–Co–P2 = 178.49(2), N1–Co–C23 = 179.46(10), N1–Co–P1 = 89.75(5), C23–Co–P2 = 90.37(1).

NMR studies). On the basis of this initial calibration, the PBE functional was selected as optimal and was used throughout this work. The calculated structure of complex **10** correlates well with the solid-state structure and confirms a triplet ground state, with an energy gap of +24.8 kcal/mol to the singlet state. The singlet ground state of **11** is also correctly predicted (though in this case the triplet state is only 3 kcal/mol higher in energy) and displays the expected square planar geometry around cobalt, with a short (essentially unactivated) N–N bond length (1.15 Å). The calculated ΔG° (at 298 K) for the equilibrium shown in Figure 11, +2.96 kcal/mol (including solvent effects), is entirely consistent with the reversible N₂ binding observed by NMR studies. This essentially thermoneutral value found by calculations lends support to a monomeric structure for **11**. The positive ΔG°_{298} observed for the formation of **11** is in sharp contrast to the calculated⁷¹ binding energy of N₂ to a closely related 4d complex, (PCP)Rh ($\Delta G^\circ_{298} = -15.8$ kcal/mol; PCP = κ^3 -[2,6-(ⁱPr₂PCH₂)₂C₆H₃][−]). The large difference in the binding of N₂ to (PCP)Rh and **10** can be partly attributed to the energetic penalty paid to enforce spin-pairing in the cobalt system ((PCP)Rh has a singlet ground state).

(b) CO. Following the partial success in binding N₂ to the cobalt center in **10**, we next tried with CO, the binding of which should be significantly more thermodynamically favored (CO is a superior σ -donor and π -acid, compared to N₂). The addition of one atmosphere of CO to a degassed C₆D₆ solution of **10** resulted in a rapid color change from green to red. Recrystallization yielded red crystals that X-ray diffraction analysis revealed to be the square planar monocarbonyl adduct PNPCo(CO), **12** (Figure 12). The solid-state structure of **12** is unremarkable, being closely similar to that of the d⁷ square planar complex **1**. Complex **12** possesses a ¹H NMR spectrum consistent with C_{2v} symmetry, a resonance in the ³¹P{¹H} NMR at 79.3 ppm and a broad singlet (from the quadrupolar, $I = 7/2$ cobalt) in the ¹³C{¹H} NMR for coordinated CO at 203.1 ppm. The infrared spectrum of crystalline **12** dissolved in pentane exhibits one sharp intense

CO stretch, $\nu_{\text{CO}} = 1885 \text{ cm}^{-1}$. This low CO stretching frequency (by comparison to that of both PNPRhCO,²² 1932 cm^{−1}, and [(ⁱPr₂P-*o*-C₆H₄)₂N]CoCO, 1901 cm^{−1})⁶⁷ confirms a significant degree of back-bonding from cobalt (again enhanced by the push–pull effect).

Interestingly, an examination of the NMR spectra of a sample of **12** under an atmosphere of CO reveals a number of differences from that recorded under argon, the most apparent being the broadening of all the resonances (to such a degree that no spin coupling is observable). The chemical shifts are unchanged from those of **10**. In addition, no resonance is observed in the ¹³C{¹H} NMR for free CO (even when isotopically enriched ¹³CO is used); these findings combined imply a fluxional process involving the coordination of CO. Dissociation of CO as source of the fluxionality (as found for the binding of N₂ to **10**) can be discounted because placing **12** under vacuum for extended periods (1 × 10^{−3} Torr, 3 days) results in no loss of CO (by ¹H and ³¹P{¹H} NMR). The fluxionality therefore must involve the association of a second molecule of CO, forming PNPCo(CO)₂, analogous to [(ⁱPr₂P-*o*-C₆H₄)₂N]Co(CO)₂.⁶⁷ The infrared spectrum of **12** in a CO-saturated pentane solution indeed confirms the presence of a second CO-containing molecule, PNPCo(CO)₂, in low concentration with two (albeit weak) stretching frequencies observed at 1840 and 1931 cm^{−1}. These CO stretches are again extremely low, especially when compared to other Co(I) dicarbonyls, for example, PhB(CH₂PⁱPr₃)₃Co(CO)₂⁴⁰ (1990 and 1904 cm^{−1}), further supporting the strongly electron-releasing properties of the PNP ligand. PNPCo(CO)₂ is observable at low temperature by NMR spectroscopy, and cooling of a sample of **12** under ~4 atm of ¹³CO to 213 K reveals a second ³¹P{¹H} NMR signal at 94.4 ppm, along with a new coordinated CO resonance in the ¹³C{¹H} NMR spectrum at 205.5 ppm (free ¹³CO is also observed at this temperature as a sharp singlet at 184.1 ppm). It is interesting that there is such a different propensity for the binding of CO between **12** and [(ⁱPr₂P-*o*-C₆H₄)₂N]CoCO (which under a CO atmosphere exists only as the dicarbonyl). Presumably this is the result of the superior electron-donating ability of the silyl amido, ^tBu PNP ligand versus the anilido ⁱPr PNP ligand. Two other four-

(71) Cohen, R.; Rytchinski, B.; Gandelman, M.; Rozenberg, H.; Martin, J. M. L.; Milstein, D. *J. Am. Chem. Soc.* **2003**, *125*, 6532.

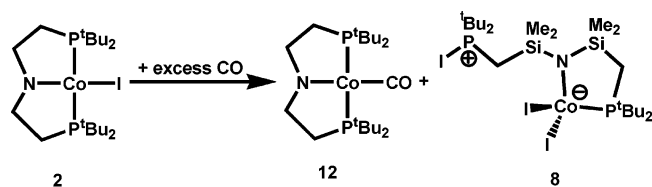


Figure 13. Reactivity of complex **2** with respect to excess CO, producing **12** and **8** (by ^1H NMR; reaction is not balanced).

coordinate monocarbonyl adducts of Co(I) have been reported, $\text{Tp}'\text{CoCo}$ ($\nu_{\text{CO}} = 1950\text{ cm}^{-1}$)⁵² and $[\text{TIMENCoCO}]^{+38}$ (1927 cm^{-1}). Both are in a distorted tetrahedral geometry, resulting in a triplet electronic ground state in contrast to square planar diamagnetic **12**, making a direct comparison of the ligand electron donating ability invalid.

Compound **12** is also produced by the reaction of excess CO with **2**, producing **8** as the only iodine-containing byproduct detected. The reduction of the cobalt center is balanced by the oxidation of a phosphine in compound **8** and not of cobalt. A similar process has been previously reported⁴⁰ with $\text{PhB}(\text{CH}_2\text{P}^i\text{Pr}_2)_3\text{CoI}$ reacting with excess CO to generate $\text{PhB}(\text{CH}_2\text{P}^i\text{Pr}_2)_3\text{Co}(\text{CO})_2$; no iodine-containing products were reported.

The reaction energy calculated (DFT) for the addition of the first CO to $(\text{PNP})\text{Co}$ is -41.0 kcal/mol , while that for the addition of CO to $(\text{PNP})\text{Co}(\text{CO})$ is only -13.3 kcal/mol , which is comparable to $T\Delta S$ at 298 K and thus is in agreement with experiment. The calculated geometry of $(\text{PNP})\text{Co}(\text{CO})_2$ is square pyramidal with CO apical and equatorial.

(c) Other Donors. Following the success with CO, the reactivity of **10** with potential ligands was investigated.⁴⁶ The addition of excess ethene to **10** was attempted, but no ethene coordination is observed even on cooling to $-60\text{ }^\circ\text{C}$, and **10** is recovered after heating in the presence of excess ethene for prolonged periods ($70\text{ }^\circ\text{C}$, C_6D_6 72 h). Ethene therefore cannot be a strong enough donor to impose spin pairing on the cobalt center. Correspondingly, no reaction was observed between **10** and excess 2-butyne. Complex **10** does react with (rigorously dried) phenyl acetylene; the major phosphorus-containing product is the free amine $\text{PN}(\text{H})\text{P}$, possibly generated by ligand protonation by the weakly acidic phenyl acetylene. Unfortunately the paramagnetic cobalt-containing products (observed in the ^1H NMR) could not be separated or purified, thereby frustrating unambiguous identification.

Conclusions

In summary, we have demonstrated that the PNP ligand set allows access to a range of low-coordinate cobalt complexes that are rigorously monomeric because of the distal steric bulk provided by four ^iBu groups, in contrast to other related, low-coordinate Co(I) and Co(II) complexes with sterically demanding ligand environments. PNPCoCl exists in equilibrium between planar ($S = 1/2$) and nonplanar ($S = 3/2$) species of energies so similar that solvent properties (not coordination to Co) can reverse the dominant species, planar ($S = 1/2$) or nonplanar ($S = 3/2$). The origin of the energetic preference for the low-spin isomer in this simple

halide species (in comparison to the $^{\text{Ph}}\text{PNP}$ derivative) was elucidated and also shown to be dominated by ligand steric bulk, with a square-planar structure maximizing phosphine substituent separation. Increasing the steric bulk of the fourth ligand substantially does not enforce a low-spin structure, with the high-spin structure being consistently observed. The Co(II) high-spin structure instead displays a large degree of ligand flexibility, with two major structural changes alleviating the steric crowding: (1) a significant opening of the P–Co–P bond (approaching the sterically preferred planar geometry) and (2) a drastic lengthening (up to 0.16 \AA compared to PNPCoCl) of the P–Co bonds.

Attempts to reach stable Co(III) complexes ligated by PNP met, counterintuitively, with limited success; simple logic dictates that the superior electron-donating phosphine with ^iBu substituents (compared to the phenyl derivative of Fryzuk) should allow greater stabilization of this higher oxidation state. Experimentally, the opposite was ascertained, with $\text{PNPCo}^{\text{III}}\text{X}_2$ complexes proving elusive, obtainable only when ligated with low electronegativity ligands (hydrides/silanes),²³ where the oxidation state formalism has less meaning. This behavior may in part be attributable to ligand non-innocence, with the presence of readily oxidized ^iBu phosphines that result in phosphorus repeatedly being the locus of oxidation. This is exemplified by the reaction of $\text{PNPCo}^{\text{II}}\text{X}$ with O_2 , which even at $-78\text{ }^\circ\text{C}$ yields a product involving phosphine oxidation and not a superoxo or peroxy species. Furthermore, the low energetic barrier (full conversion by $-78\text{ }^\circ\text{C}$) to phosphine oxidation repeatedly observed, despite the coordinated P^{III} having no available lone pair, implies a labile $\text{Co}^{\text{II}}\text{--P}$ bond.⁷²

The Co^I oxidation state is easily obtained from PNPCoX and any number of reducing agents with the resultant three-coordinate PNPCo complex shown to be T-shaped and have a triplet ground state. Weak nucleophiles show no or limited propensity to bind in the vacant fourth site, implying that any new Co–L bonds will have to provide significant binding energy to overcome that required to induce electron pairing. The cobalt center in PNPCo was found to be extremely electron rich (by IR spectroscopy of its carbonyl); in comparison to other pincer ligands, PNP builds the most reducing power into $(\text{pincer})\text{M}$ yielding²³ dihydride $\text{PNPCo}^{\text{III}}\text{--}(\text{H})_2$, not dihydrogen. The redox properties of the electron-rich PNPCo are however paradoxical; while one electron oxidation of cobalt readily occurred, there was a reluctance for full two electron-transfer that would result in Co^{III} . To a degree this failure (and the related inability to produce PNPCoH from reaction with H atom donors) is caused by the reducing power of PNPCo being strongly dependent on not only the redox potential of cobalt but also, equally importantly, on the energy recouped in the formation of new Co–X bonds.

Overall this work with O_2 and I_2 highlights a current common theme, that of ligand non-innocence, which in the $^i\text{BuPNP}$ ligand set is evident at both the labile, oxidizable

(72) Fryzuk, M. D.; Carter, A.; Rettig, S. J. *Organometallics* **1992**, *11*, 469.

phosphine functionalities. These ligand vulnerabilities need to be considered when attempting to install any electrophilic reactive functionality at the metal center. Certainly every ligand has its vulnerabilities.^{73–75}

Experimental Section

General Considerations. All manipulations were performed using standard Schlenk techniques or in an argon-filled glovebox. Solvents were distilled from Na/benzophenone, CaH₂, or 4 Å molecular sieves, degassed prior to use and stored in airtight vessels. All reagents were used as received from commercial vendors or synthesized by published routes. PNPMgCl/dioxane (PNP = [(^tBu₂PCH₂SiMe₂)₂N][−]) was prepared according to literature methods. ¹H NMR chemical shifts are reported in ppm relative to protio impurities in the deuterated solvents. ³¹P{¹H} spectra are referenced to external standards of 85% H₃PO₄ (at 0 ppm); ²⁹Si and ²⁹Si{¹H} spectra are referenced to external standards of (CH₃)₄Si (at 0 ppm). NMR spectra were recorded with a Varian Gemini 2000 (300 MHz, ¹H; 121 MHz, ³¹P; 75 MHz, ¹³C), a 400 MHz Varian Unity Inova (400 MHz, ¹H; 162 MHz, ³¹P; 101 MHz, ¹³C), or a 500 MHz Varian Inova instrument (500 MHz, ¹H; 99 MHz, ²⁹Si). Solution magnetic moments were recorded at 25 °C (unless otherwise stated) using the Evans method. Consistently for these paramagnetic complexes, no ³¹P{¹H} was observable. Infrared spectra were recorded on a Nicolet 510P FT-IR spectrometer.

PNPCoCl (1). Compound **1** was synthesized in a closely related manner to that reported for the phenyl derivative, (Ph₂PCH₂SiMe₂)₂-NCoCl.²⁷ PNPMgCl/dioxane (1.6 g, 2.7 mmol) was dissolved in 40 mL of THF, and 1.05 equiv of anhydrous CoCl₂ (0.365 g, 2.8 mmol) was added as a solid. The solution rapidly turned deep blue. After the mixture was stirred for 18 h, the THF was removed in vacuo; the resulting oil was dissolved in toluene and filtered, and the volume was reduced to ~5 mL. Cooling of the mixture to −40 °C overnight yielded 0.800 g of a red crystalline product. The filtrate was reduced to dryness in vacuo, redissolved in minimum pentane, and cooled overnight at −40 °C to yield a second crop (0.260 g) of red crystals. Combined yield: 73% (1.06 g, 1.9 mmol). ¹H NMR (298 K, C₆D₆): δ 30.4 (4H, v. broad singlet), 8.2 (12H, v. broad singlet) 2.6 (36H, v. broad singlet). Magnetic moment (Evans method, 298 K, C₆D₆): 3.96 μ_B. ¹H NMR (298 K, C₆D₁₂): δ 15.98 (4H, broad singlet), 3.01 (36H, broad singlet) 1.08 (12H, broad singlet). Magnetic moment (Evans method, C₆D₁₂): 2.85 μ_B. ¹H NMR (298K, C₇D₈): δ 27.0 (4H, broad singlet), 7.1 (broad singlet, overlapped with protio toluene making an accurate integration impossible), 2.6 (36H, broad singlet). Magnetic moment (C₇D₈): 3.21 μ_B.

Attempts to record a mass spectrum of Complex **1** repeatedly failed, with the major molecular ion observed corresponding to **P(O)NP(O)CoCl** [M + 1]⁺.

PNPCoI (2). PNPMgCl/dioxane (1.5 g, 2.5 mmol) was dissolved in 30 mL of THF, and 1.05 equiv of anhydrous CoI₂ (0.825 g, 2.6 mmol) was added as a solid. The solution rapidly turned turquoise. After the mixture was stirred for 18 h, the THF was removed in vacuo; the resulting oil was dissolved in toluene and filtered, and the volume was reduced to ~5 mL. Cooling to −40 °C overnight yielded 0.850 g (1.4 mmol) of turquoise crystalline product. Yield: 54%. ¹H NMR (298 K, C₆D₆): δ 63.73 (4H, broad

singlet), 19.49 (12H, broad singlet) 1.94 (36H, broad singlet). Magnetic moment (C₆D₆): 4.54 μ_B. ¹H NMR (298 K, C₆D₁₂): δ 59.57 (4H, broad singlet), 18.30 (12H, broad singlet), 1.66 (br singlet, accurate integration was impossible because of the overlap of the signal with residual protio cyclohexane). Magnetic moment (C₆D₁₂): 5.05 μ_B.

PNPCoN₃ (3). A Schlenk flask was charged with PNPCoCl (0.400 g, 0.74 mmol) and 15 mL of THF; 10 equiv of NaN₃ (0.481 g, 7.4 mmol) was added as a solid. After it was stirred overnight, the solution changed color from deep blue to terracotta; the THF was removed in vacuo, and the resultant oil was redissolved in pentane and filtered. The pentane was reduced to minimum volume. Storage of the mixture at −40 °C for 3 days yielded red crystals (0.303 g, 0.55 mmol). Yield: 74%. ¹H NMR (298 K, C₆D₆): δ 6.5 (4H, broad singlet), 2.4 (36H, broad singlet) −4.0 (12H, broad singlet). Magnetic moment (C₆D₆): 2.47 μ_B. IR (cm^{−1}, pentane): ν 2081.

PNPCoNH(2,6-Me₂-C₆H₃) (4). A Schlenk flask was charged with PNPCoCl (0.126 g, 0.23 mmol) and 10 mL of THF to yield a deep blue solution; 1.05 equiv of LiNH(2,6-Me₂-C₆H₃) (0.031 g, 0.24 mmol) was then added as a solid, resulting in a rapid color change to purple. The solution was stirred for a further 4 h before the THF was removed in vacuo. The resultant purple oil was redissolved in toluene and filtered; the toluene was removed in vacuo, and the oil was redissolved in a minimum amount of pentane and cooled to −40 °C for 18 h to yield purple crystals (0.090 g, 0.14 mmol). Yield: 62%. ¹H NMR (298 K, C₆D₆): δ 12.49 (4H br singlet), 10.07 (48H, br singlet of 4 tBu and 4 SiMe), −88.72 (6H, br singlet of anilido methyls). The phenyl ring protons are not observed in the region of +150 to −150 ppm. Magnetic moment (C₆D₆): 4.28 μ_B.

P(O)NP(O)CoCl (5). In a standard reaction, a Youngs NMR tube was charged with 0.015 g of PNPCoCl and 0.45 mL of C₆D₆ and transferred to a gas line. The deep blue solution was degassed twice (freeze/pump/thaw) and refilled with an atmosphere of O₂. When it thawed, a rapid color change was observed from deep blue to royal blue, and the ¹H NMR spectrum showed the quantitative conversion to a single new C_s symmetric paramagnetic product. Alternatively P(O)NP(O)CoCl can be synthesized quantitatively by the addition of 2.1 equiv of PhI=O (iodosobenzene) to PNPCoCl in C₆D₆, with PhI observed as the byproduct. Yield: Quantitative by NMR. ¹H NMR (298 K, C₆D₆): δ 24.30 (6H, singlet), 11.61 (2H, singlet) 0.11 (18H, singlet), −3.53 (18H singlet), −14.10 (6H, singlet), −21.65 (2H, singlet). Magnetic moment (C₆D₆): 4.50 μ_B. MS (ESI+) Calcd for C₂₂H₅₂Si₂P₂N₁O₂Co₁Cl₁: 574.2. Found (M + 1): 575.1.

P(O)NP(O)CoI (6). In a standard reaction, a Youngs NMR tube was charged with 0.010 g of PNPCoI and 0.45 mL of C₆D₆ and transferred to a gas line. The turquoise solution was degassed twice (freeze/pump/thaw) and refilled with an atmosphere of O₂. When thawed, a rapid color change was observed from deep blue to royal blue, and the ¹H NMR spectrum showed the quantitative conversion to a single new C_s symmetric paramagnetic product. Alternatively P(O)NP(O)CoI can be synthesized quantitatively by the addition of 2.1 equiv of PhI=O to PNPCoI in C₆D₆, with PhI observed as the byproduct. Yield: Quantitative by NMR. ¹H NMR (298 K, C₆D₆): δ 24.05 (6H, singlet), 11.09 (2H, singlet) −0.23 (18H, singlet), −2.15 (18H singlet), −15.13 (6H, singlet) and −23.57 (2H, singlet). MS (ESI+) Calcd for C₂₂H₅₂Si₂P₂N₁O₂Co₁I₁: 666.1. Found (M + 1): 667.3.

P(O)NP(O)CoN₃ (7). In a standard reaction, a Youngs NMR tube was charged with 0.015 g of PNPCoN₃ and 0.45 mL of C₆D₆ and transferred to a gas line. The red solution was degassed twice

(73) Ben-Ari, E.; Leitus, G.; Shimon, L. J. W.; Milstein, D. *J. Am. Chem. Soc.* **2006**, *128*, 15390.

(74) Scott, J.; Gambarotta, S.; Korobkov, I.; Budzelaar, P. H. M. *J. Am. Chem. Soc.* **2005**, *127*, 13019.

(75) Collins, T. J. *Acc. Chem. Res.* **1994**, *27*, 279.

(freeze/pump/thaw cycles) and refilled with an atmosphere of O₂. When thawed, a rapid color change was observed from red to blue, and ¹H NMR spectrum showed the quantitative conversion to a single new C_s symmetric paramagnetic product, crystals of which could be obtained by the slow evaporation of a benzene solution. Yield: Quantitative by NMR. ¹H NMR (298 K, C₆D₆): δ 25.24 (6H, singlet), 11.55 (2H, singlet), 1.14 (18H, singlet), -4.59 (18H singlet), -14.01 (6H, singlet), -21.87 (2H, singlet). IR (cm⁻¹, KBr): 2058.

PNP(I)CoI₂ (8). A Schlenk flask was charged with PNPCo (0.050 g, 0.1 mmol) and dissolved in 3 mL of C₆H₆; 2 equiv of I₂ (0.025 g, 0.2 mmol) dissolved in C₆H₆ was then added dropwise while stirring. The solution rapidly changed color from green to pale blue. After the mixture was left standing for several minutes a pale blue microcrystalline solid precipitated from solution (0.068 g, 0.077 mmol). An alternative synthesis starting from PNPCoI and 1.1 equiv of I₂ quantitatively yields **8** (by NMR). Yield: 77%. ¹H NMR (298 K, THF-*d*₈): δ 56.35 (2H, br s), 27.58 (6H, br s), 15.26 (6H, br s), 1.12 (18H br s), -6.46 (18H, s), -72.36 (2H, v. br s). ³¹P{¹H} NMR (298 K, THF-*d*₈): δ 269.5 (br s). Magnetic moment (THF-*d*₈): 4.78 μ_B. MS (ESI⁻): Molecular ion not observed, instead [M - I]⁻ (calcd for C₂₂H₅₂NP₂Si₂CoI₂, 761.1; found, 761.2) and [M - 'Bu]⁻ (calcd for C₁₈H₄₃NP₂Si₂CoI₃, 830.9; found, 831.0).

PNPCoCl + TMSOTf, forming PNPCo(OTf) (9). A J. Youngs tube was charged with 15 mg of PNPCoCl and 1 mL of C₆H₆, and 100 equiv of TMSOTf was then added. Slow evaporation of benzene yielded two distinct sets of crystals: red crystals (confirmed as **1** by X-ray crystallography) and dark blue crystals. Mechanical separation of the crystals leads to a predominantly pure sample of **9** with only minor contamination from **1**. Attempts to record a magnetic moment (Evans method) for this sample were frustrated by the inability to obtain useful analytically pure amounts. ¹H NMR (298 K, C₆D₆): δ 43.3 (4H, broad singlet), 17.7 (36H, broad singlet), -5.4 (12H, broad singlet).

PNPCo (10). PNPCoCl (0.500 g, 0.92 mmol) was loaded into a Schlenk flask and dissolved in 30 mL of THF. Magnesium powder (25 equiv, 0.560 g, 23 mmol) was added as a solid to the deep blue solution and stirred for 18 h. The resulting green solution was reduced to dryness in vacuo, redissolved in toluene (20 mL) filtered,

and reduced to dryness to give a green solid. Redissolution in minimum toluene and cooling to -40 °C yielded, upon isolation, 0.310 g of green crystals. The remaining filtrate was reduced in volume and cooled to -40 °C for 24 h to yield a second crop of green crystals (0.065 g). Combined Yield: 76% (0.375 g, 0.74 mmol). ¹H NMR (C₆D₆, 298 K): δ 12.5 (36H, s), 0.30 (12H, s), -24.2 (4H, s). ¹³C{¹H} NMR (C₆D₆, 298 K): δ 272 (s), 253 (s), 234 (br s), 101 (br s). Magnetic Moment (C₆D₆): 3.2 μ_B.

PNPCo(N₂) (11). A J. Youngs NMR tube was charged with PNPCo (0.020 g, 0.04 mmol) that was dissolved in 0.45 mL of toluene-*d*₈. On a gas line, the green solution was degassed three times by freeze/pump/thaw cycles and charged with N₂ at 77 K (~4 atm). ¹H NMR (223 K, toluene-*d*₈): δ 1.39 (s, 36H), 1.12 (s, 4H), 0.32 (s, 12H). ³¹P{¹H} NMR (223 K, toluene-*d*₈): δ 66.3 (s). IR (298 K, cm⁻¹, N₂ saturated pentane solution): 2004 (s).

PNPCo(CO) (12). A flask with a Teflon cap was charged with PNPCo (0.550 g, 1.1 mmol) and 10 mL of pentane and transferred to a gas line. The solution was degassed three times (freeze/pump/thaw cycles) and backfilled with 1 atm of CO. When thawed, the solution immediately turned from green to red. The pentane was removed in vacuo, and the resultant red crystalline solid (0.464 g, 0.87mmol) was analytically pure. The CO is not removable after evacuation at 25 °C (at 5 Torr) after 18 h. Yield: 80%. ¹H NMR (298 K, C₇D₈): δ 1.34 (36H, t, 6.3 Hz), 0.84 (4H t, 4.5 Hz), 0.25 (12H, br s). ³¹P{¹H} NMR (298 K, C₇D₈): δ 79.3 (s). ¹³C{¹H} NMR (298 K, C₇D₈): δ 203.1 (br s), 35.5 (s), 29.8 (s), 10.7 (s), 5.92 (s). IR (cm⁻¹, pentane): 1885.

Acknowledgment. This work was supported by the NSF (CHE-0544829). Professors Mu-Hyun Baik and Daniel Mindiola are thanked for useful discussions.

Supporting Information Available: Computational details, optimized structures of (PNP)Co, (PNP)Co(N₂), (PNP)Co(CO), (PNP)Co(CO)₂, (PNP)CoCl, selected bond distances and angles, SOMOs, and full crystallographic details. This material is available free of charge via the Internet at <http://pubs.acs.org>.

IC701171P